THE HIGHLY SIDEROPHILE ELEMENT COMPOSITION OF THE LUNAR MANTLE. James M.D. Day[1] and Richard J. Walker[2], [1]Geosciences Research Division, Scripps Institution of Oceanography, La Jolla, CA 92093 (jmdday@ucsd.edu); [2]Department of Geology, University of Maryland, College Park, MD 20742.

Introduction: Derivative melts of the Moon's interior, sampled as mare basalts and pyroclastic glass beads represent the only available materials for establishing lunar mantle composition. Pyroclastic glasses are believed to represent primitive (13-20 wt.% MgO) high-degree partial melts sourced from the deep mantle (>400 km [1]), whereas mare basalts have witnessed more complex petrogenetic histories (e.g., [2,3]). In terrestrial igneous systems, high-MgO melts, such as picrites and komatiites have highly siderophile element (HSE) abundances most similar to their mantle sources because they result from high degree partial melting, with (nearly) all sulphide in the parent mantle being incorporated into the melt (e.g. [4]). Following this rationale, early studies concluded that the Ir contents of picritic high-Ti orange and low-Ti green glasses were only offset from the terrestrial array by a factor of 2 to 4 [5,6], leading some authors to conclude that the abundances of HSE in the lunar mantle sampled by picritic glasses are similar to those in the terrestrial mantle [7]. If true, these glasses would provide an entirely different view of lunar mantle differentiation than indicated by the HSE abundances of mare basalts [8]. Here we evaluate the current evidence for establishing lunar mantle HSE abundances and consider these elements in the context of models for lunar evolution.

Picritic Glass Beads: Pristine pyroclastic picritic glasses [9] contain elevated volatile and siderophile abundances that are surface-correlated (e.g., [10,11]). Although models of fire-fountaining by CO generation from graphite (e.g., [12]) can explain some of the surface-correlated features of the picritic glass beads (e.g., deposition of volatile Zn, S, Cl, F, Pb, and Zn isotope fractionation [13], as well as reduction of FeO to Fe metal [14]), such models do not explain vapour deposits found on fracture surfaces [15], or surface-correlated HSE enrichments [6,10,11,16,17]. Walker et al. [17] showed that etchates, derived from the outer surfaces of the beads and representing 5-30% of their volume, have chondritic-relative abundances of the HSE and near-chondritic $^{187}Os/^{188}Os$, whereas the residues, which represent the interior of the beads, have distinctly non-chondritic relative HSE abundances and $^{187}Os/^{188}Os$, with HSE abundances more akin to high-MgO mare basalts [8]. Surface-correlated elevated HSE abundances have been ascribed to meteoritic contamination on the outer surfaces of the glass beads after their formation and emplacement [17], casting doubt on the picritic glass beads as deriving from a lunar mantle reservoir with similar HSE abundances to those found in the terrestrial mantle (e.g., [7]) and supporting derivation from a lunar mantle source with HSE abundances similar to those estimated for high- and low-Ti mare basalts, at ≤0.0004 × CI-chondrites [8].

Mare Basalts: Apollo 12, 15 and 17 mare basalts, and mare basalt meteorites have HSE abundances (~1×10^{-3} to 1×10^{-7} times CI-chondrite) that extend the range of abundances measured for picritic glass bead interiors (~1×10^{-3} to 1×10^{-5} times CI-chondrite [17]) and exhibit relatively flat chondrite-relative HSE patterns, to patterns that are strongly fractionated (Fig. 1).

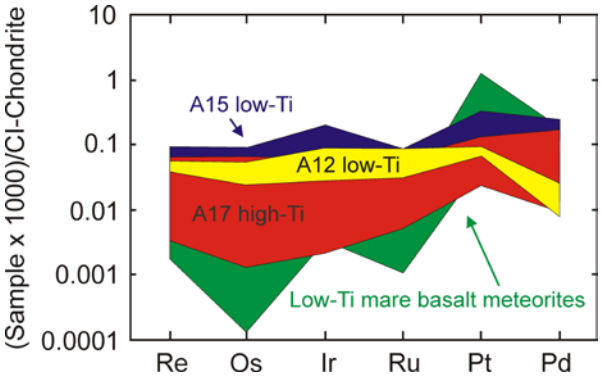

Figure 1: *Fields of HSE patterns for mare basalts normalized to CI-chondrite, Orgueil [19]. Data from this study and [8].*

With few exceptions, mantle-derived terrestrial basalts of similar MgO contents exhibit higher HSE abundances than those measured for mare basalts (e.g., [18]). Low HSE abundances in S-undersaturated lunar mare basalts cannot be explained by volatile loss during eruption, as proposed for Re in some terrestrial lavas (e.g., [18]). Osmium abundances show a broadly positive correlation with MgO, and mare basalts with low MgO contents (<6.5-9 wt.%) typically have higher $^{187}Os/^{188}Os$ (up to 0.513) than high MgO mare basalts (from 9->16.5 wt.%) that have $^{187}Os/^{188}Os$ (0.1215-0.160) broadly in the range of chondrites. Fractionated HSE patterns that correlate with decreasing MgO and HSE abundances are consistent with fractional crystallization and removal of Os, Ir and Ru in early crystallizing phases (olivine ± chromite; armalcoite for some high-Ti basalts?), relative to Pt, Pd and Re.

Lunar Mantle HSE Abundance Estimates: Day et al. [8] utilized the relationship of HSE abundance variations with indices of fractionation (e.g., MgO) in mare basalts to perform regression analysis to an esti-

mated lunar mantle composition. The estimated mantle concentrations obtained (0.01 ng g^{-1} Re, 0.1 ng g^{-1} Os, Ir, Ru, Pd and 0.2 ng g^{-1} Pt) are more than 20 times lower than HSE abundances estimated for Earth's primitive mantle [20]. Low concentrations of the HSE in the lunar mantle are supported by ultra-low HSE abundances measured in pristine lunar crustal rocks [21], indicating a bulk silicate Moon with significantly lower HSE abundances than for bulk silicate Earth.

Two unconstrained aspects of lunar mare basalt genesis currently limit our ability to more accurately estimate lunar mantle composition. First, contamination of mare basalt lavas by even minor amounts (<0.01% by mass) of HSE-rich impactor material residing on the lunar surface (e.g., [22]) would lead to increased HSE contents, flatter HSE patterns and chondritic $^{187}Os/^{188}Os$. Given the existing dataset (Fig. 1), this process would need to act most effectively on high-MgO lavas, relative to low-MgO lavas, and means that any estimates of lunar HSE abundance for the lunar mantle represent maximum estimates (c.f., [8]). Second, residual metal after melt extraction at low fO_2 conditions in the lunar mantle would lead to strongly fractionated HSE inter-element ratios, and significant $^{187}Os/^{188}Os$ variation would be established from the time of mantle source crystallization (>4.4 Ga) to the eruption of mare basalts (~3.8-3.0 Ga). The observation of the highest HSE abundances in lavas with the highest MgO, and the relatively low degrees (~10-15% [8]) of partial melting estimated for mare basalts make the possibility of residual metal acting on resultant melt compositions unlikely. Despite these limitations, establishment of lunar mantle HSE concentrations, by use of HSE-MgO regressions, or HSE inter-element ratios (assuming chondritic proportions [20]) yields lunar mantle HSE abundances that are >20 × lower than HSE abundances in the terrestrial mantle.

Lunar mantle HSE heterogeneity? The lunar mantle is inhomogeneous, with evidence for mineralogical heterogeneity and fractionation of stable isotopes (e.g., Li, O, Fe [23-25]), as well as fractionation of the long-lived Rb-Sr, Sm-Nd, Lu-Hf and U-Th-Pb isotope systems in mare basalt source regions. Mantle heterogeneity is considered to result from magma-ocean crystallization and generation of cumulate mantle [26], followed by overturn and mixing of the cumulate layers because of gravitational instability [27]. Therefore, a caveat of lunar mantle HSE abundance estimates is that they may not represent the distribution of these elements in the lunar mantle as a whole. Understanding the distribution of the HSE is important since magma ocean differentiation might be expected to lead to strong HSE fractionation, depending on the timing of late accretion additions to the Moon. Mineralogy, major- and trace-element abundances and O-Fe-Sr-Nd-Hf isotopes for samples measured for HSE abundances and $^{187}Os/^{188}Os$ support derivation of these samples from heterogeneous mantle source regions, yet HSE abundances estimated for low- and high-Ti mare basalt sources are broadly similar.

The similarity of HSE abundances measured for low- and high-Ti mare basalts measured thus far offer some support for a lunar mantle that had relatively homogeneous distribution of the HSE, in chondritic relative proportions, but more data are required to test this hypothesis. At face-value, the current HSE abundance data for lunar derivative melts support their derivation from a lunar mantle that witnessed limited post-core formation late accretion with respect to the HSE [8], but that lunar mantle differentiation did not lead to strong HSE fractionation, and may even have acted to establish relatively homogenized lunar mantle HSE abundances, in the same manner that mantle convection on Earth is believed to have homogenized the HSE. Constraints from lunar crust formation ages [28], and HSE abundances [21] require a limited time-frame (<100 Ma after Earth-Moon formation) for post-core formation late accretion and lunar differentiation, with the addition of chondritic relative abundances of the HSE to the lunar mantle by one or a few large (250-300 km diameter) impactors [29].

Acknowledgements: We are grateful to CAPTEM and the JSC curation staff for provision of samples. This research was partially supported by NASA LASER grant (NNX11AB20G).

References: [1] Shearer & Papike (1993) *GCA*, **57**, 4785 [2] Neal & Taylor (1992) *GCA*, **56**, 2177 [3] Longhi (2006) *GCA*, **70**, 5919 [4] Walker (2009) *Chem. Erde*, **69**, 101 [5] Ganapathy et al. (1973) *PLSC*, **4**, 1239 [6] Morgan & Wandless (1979) *PLPSC*, **10**, 327 [7] Ringwood (1992) *EPSL*, **111**, 537 [8] Day et al. (2007) *Science*, **315**, 217 [9] Delano (1986) *JGR,* **91**, D201 [10] Chou et al. (1975) *PLSC*, **6**, 1701 [11] Krahenbuhl (1980) *PLPSC*, **11**, 1551 [12] Fogel & Rutherford (1995) *GCA*, **59**, 201 [13] Herzog et al. (2009) *GCA*, **73**, 5884 [14] Weitz et al. (1999) *M&PS*, **34**, 547 [15] Cirlin & Housley (1979) *PLPSC,* **10**, 341 [16] Wasson et al. (1976) *PLSC*, **7**, 1583 [17] Walker et al. (2004) *EPSL*, **224**, 399 [18] Day et al. (2010) *GCA*, **74**, 6565 [19] Horan et al. (2003) *Chem. Geol.* **196**, 5 [20] Becker et al. (2006) *GCA,* **70**, 4528 [21] Day et al. (2010) *EPSL,* **289**, 595 [22] Puchtel et al. (2008) *GCA,* **72**, 3022 [23] Spicuzza et al. (2007) *EPSL*, **253**, 254 [24] Day et al. (2008) *LPSC*, **39**, 1072 [25] Liu et al. (2010) *GCA*, **74**, 6249 [26] Wood et al. (1970) *PLSC*, **1**, 965 [27] Elkins-Tanton et al. (2002) *EPSL,* **196**, 239 [28] Norman et al. (2003) *M&PS,* **38**, 645 [29] Bottke et al. (2010) *Science,* **330**, 1527.